Journal of
Mechanical
Science and
Technology

Journal of Mechanical Science and Technology 21 (2007) 455~464

Prediction of Actuating Displacement in a Piezoelectric Composite Actuator with a Thin Sandwiched PZT Plate by a Finite Element Simulation

Sung-Choong Woo[a], Nam Seo Goo[b,*]

[a]*Artificial Muscle Research Center, Konkuk University, 1 Hwayang-dong, Gwangjin-gu, Seoul 143-701, Korea*
[b]*Intelligent Microsystem Program, Department of Advanced Technology Fusion, Konkuk University, 1 Hwayang-dong, Gwangjin-gu, Seoul 143-701, Korea*

(Manuscript Received June 30, 2006; Revised December 15, 2006; Accepted January 10, 2007)

Abstract

This paper presents the evaluation of a plate-type piezoelectric composite actuator (PCA) with a thin sandwiched plate having four kinds of lay-up configurations by analyzing the flexural displacement. For this, a three-dimensional finite element simulation considering the thermal deformation effect of PCA during manufacturing is conducted based on a thermal analogy model. The distribution of residual thermal stresses and the dome height caused by the mismatch in coefficient of thermal expansion (CTE) between the layers of PCA are predicted with the aid of a classical laminated plate theory (CLPT). Results of finite element analyses have revealed that the flexural displacement of PCA subjected to electric fields is considerably affected by the variation of lay-up configuration, the thickness of an embedded PZT wafer and boundary conditions. In particular, as the thickness of the PZT ceramic increases, the bending stiffness of PCA increases faster than the actuation distance does, which leads to the overall reduction in flexural displacement. It is therefore suggested that the electrically induced flexural displacement of unimorph-type PCA depends more on the bending stiffness than on the actuation distance.

Keywords: Piezoelectric composite actuator, Flexural displacement, Thermal deformation, Bending stiffness

1. Introduction

Piezoelectricity is the property of a material by which a voltage is produced as a result of a mechanical force, and conversely a mechanical deformation ensues when a voltage is applied. Piezoelectric materials, such as the lead zirconate titanate (PZT) and the polyvinylidene fluorides (PVDF), are generally used in the form of thin layer. The former which is a ceramic genealogy is commonly used as an actuator due to a high actuating force for low applying electric fields. The latter which is a polymer genealogy is mainly applied to a sensor because of the high voltage generation for a small deformation.

During the last several years, piezoelectric actuators have received considerable amount of attention in the field of shape/vibration control (Hwang et al., 1993; Tzou et al., 1995) and light-weight aerospace structures on account of design flexibility together with high force and large displacement performances. In addi-tion, piezoelectric actuators have a potential utiliza-tion in a variety of applications such as micropumps (Teymoori et al., 2005) for drug delivery in the medical industry based on MEMS technology and synthetic jet actuators (Liang et al., 2005) which control the stall induced by air separation on the wing

*Corresponding author. Tel.: +82 2 450 4133; Fax.: +82 2 444 7091
E-mail address: nsgoo@konkuk.ac.kr

surface. Many of piezoelectric actuator devices are unimorph-type, in which a PZT ceramic is bonded to and/or embedded into thin metal and fiber composite layers. Haertling (1994) introduced RAINBOW (Reduced And INternally Biased Oxide Wafer) transducer/actuator using hybrid concept. After that, NASA developed THUNDER (THin-layer Unimorph ferroelectric DrivER) (Hellbaum et al., 1997) combining metal layer of substrate with thin PZT ceramic layer. According to the studies on RAINBOW and THUNDER, thermally induced residual stresses play an enhancing role in the actuating performance (Wise, 1998).

Analyses of composite structures containing PZT ceramic have been documented in the literature. Mulling et al. (2001) investigated the actuating capability of THUNDER as a function of load at various boundary conditions and reported that restrictive end conditions increased small amount of stiffness enhancing the load capabilities of THUNDER. Yoon and coworkers (Goo et al., 2001; Yoon et al., 2004; Kim et al., 2005) developed LIPCA (LIght weight Piezo-composite Curved Act-uator, see the Fig. 1(a)) replacing the metal layer in THUNDER by fiber composite and explained the actuating principle of LIPCA in a simple and analytic manner. It was reported that LIPCA was much lighter by 34 % and had much better actuating performance by 13 % compared with THUNDER7-R model. Haris et al. (2004) defined an actuation coefficient and studied the influence of the initial dome height and bending stiffness on the actuating performance using a simple analytic and numerical model based on beam theory for predicting the displacement of the LIPCA. Recently, Gex et al. (2005) manufactured a bending piezoelectric actuator termed GEPAC with a 250 μm thick PZT plate embedded in five layers of unidirectional Kevlar-epoxy. It was shown in their study that by segmenting the top electrode, it was possible to perform ultrasonic NDE health monitoring of the actuator itself simultaneously with the low frequency actuation. Since the shape of above mentioned piezoelectric actuators is a beam model whose length to width ratio is large, anticlastic curvature as shown in Fig. 1(b) due to the CTE mismatch between the layers has hardly influences on the actuating perfor-mance of piezoelectric actuators. However, in the case of rectangular or square type actuators whose length to width ratio is small, the saddle shaped curvature may lead to the reduction in the actuating performance and the degradation in their integrity. Also, the thermal deformations induced by a tem-perature variation during the curing process should be considered for a more exact performance evaluation. This work is the third of a series of reports. The first work (Woo et al., 2006a, 2007) experimentally discussed the effects of applied electric fields and drive fre-quencies on the flexural displacement of a plate-type piezoelectric composite actuator (PCA). The second paper (Woo et al., 2006b) evaluated the integrity of PCA subjected to a mechanical bending load with the aid of acoustic emission non-destructive technique in relation to the macroscopic and microscopic bending fracture process.

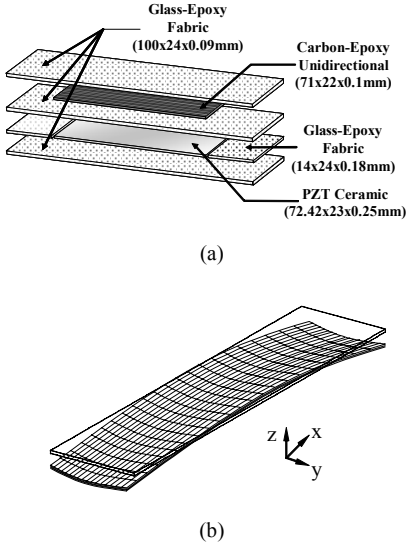

Fig. 1. (a) The lay-up sequence of the LIPCA-C2 and (b) its deformed shape with an anticlastic curvature due to CTE mismatch after curing.

In this work, in an attempt to confirm the applicability of PCA to pumping devices or synthetic jet actuators, the flexural displacement of PCA having four different lay-up configurations has been evaluated under various boundary conditions; the effects of lay-up sequence and the thickness of PZT ceramic on the displacement performance of PCA are elucidated in association with the bending stiffness and the actuation distance of PCA. Classical laminated plate theory (CLPT) is adopted to obtain the distribution of residual stresses in the respective layer. To predict the flexural displacement of PCA, three dimensional finite element analysis based on thermal analogy model is

conducted with the commercial code pro-gram ANSYS.

2. Theoretical considerations

2.1. Laminated plate theory for the design of a piezoelectric composite actuator

Thermally-induced residual stresses in the curing process have influence not only on the integrity of piezoelectric composite actuator but also on its actuating performance (Cho et al., 1998). Since it is widely accepted that the PZT ceramic breaks easily under tensile stress as compared to the compressive stress, it is desirable that only compressive residual stress should be applied to the PZT ceramic layer (Mossi et al., 2005).

The distribution of residual thermal stresses in each layer of PCA is investigated using a classical laminated plate theory. As shown in Fig. 2, four kinds of lay-up type are adopted and Table 1 presents material properties used for this study. In this study, some assumptions are made. First, PZT ceramic is a transversely isotropic material ($d_{31} = d_{32}$) and there are no shearing forces induced by piezoelectricity ($d_{36} = 0$). Second, each layer is perfectly bonded to one another. Third, the thickness of the laminated plate is sufficiently small compared to its length and width (plane stress condition).

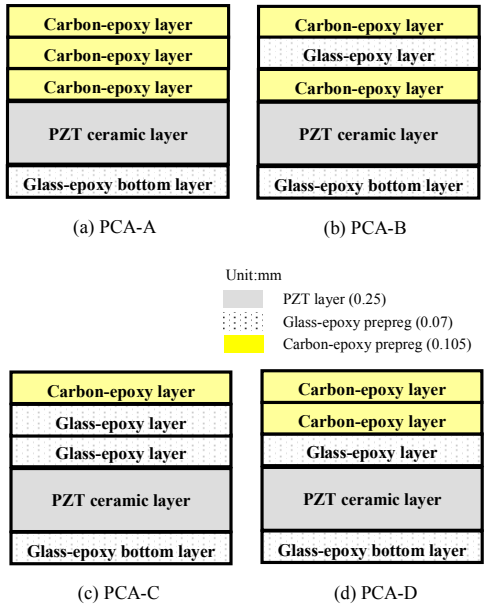

Fig. 2. Schematic of plate-type piezoelectric composite actuators according to different lay-up sequences.

The linear constitutive stress-strain relations for a laminated composite plate with a PZT layer are expressed as follows

$$\varepsilon_i = S_{ij}\sigma_j + d_{ik}E_k + \alpha_i \Delta T \tag{1}$$

where σ_j and ε_i are the stress and strain component respectively; E_k and S_{ij} the electric field and compliance coefficients; d_{ik}, α_i and ΔT piezoelectric strain constants, coefficients of thermal expansion and temperature change from the reference temperature, respectively.

The converse form of Eq. (1) for the k^{th} ply in the laminate coordinates can be expressed as following

$$\begin{Bmatrix}\sigma_x\\ \sigma_y\\ \tau_{xy}\end{Bmatrix}^k = \begin{bmatrix}\overline{Q}_{11} & \overline{Q}_{12} & \overline{Q}_{16}\\ \overline{Q}_{12} & \overline{Q}_{22} & \overline{Q}_{26}\\ \overline{Q}_{16} & \overline{Q}_{26} & \overline{Q}_{66}\end{bmatrix}^k \left\{\begin{pmatrix}\varepsilon_x^0\\ \varepsilon_y^0\\ \gamma_{xy}^0\end{pmatrix} + \begin{pmatrix}\kappa_x\\ \kappa_y\\ \kappa_{xy}\end{pmatrix} z - \begin{pmatrix}d_{31}\\ d_{32}\\ 0\end{pmatrix} E_z - \begin{pmatrix}\alpha_x\\ \alpha_y\\ \alpha_{xy}\end{pmatrix} \Delta T\right\}^k \tag{2}$$

where $\overline{Q}_{ij}$, ε^o and κ are the transformed reduced stiffness, mid-plane strain and curvature. The transformed stiffness and coefficients of thermal expansion are

$$[\overline{Q}_{ij}] = [T]^{-1}[Q_{ij}][T]^{-T} \tag{3}$$

$$[\overline{\alpha}] = [T]^{-1}[\alpha] \tag{4}$$

where the transformation matrix is given by

$$[T] = \begin{bmatrix} m^2 & n^2 & 2mn \\ n^2 & m^2 & -2mn \\ -mn & mn & m^2 - n^2 \end{bmatrix} \tag{5}$$

In Eq. (5), the terms m and n are $cos\theta$ and $sin\theta$ respectively where θ is the angle between the global axis and the fiber orientation of lamina.

Integrating Eq. (2) over the total thickness of laminate and then force and moment resultants are obtained as

$$\begin{bmatrix} A & B \\ B & D \end{bmatrix} \begin{Bmatrix} \varepsilon^o \\ \kappa \end{Bmatrix} = \begin{Bmatrix} N^{mech} + N^{elec} + N^{thermal} \\ M^{mech} + M^{elec} + M^{thermal} \end{Bmatrix} \tag{6}$$

where A, B and D are the extensional stiffness, bending-extensional coupling stiffness and bending stiffness matrix respectively, which are defined in terms of the lamina stiffness $\overline{Q}_{ijk}$ as

$$A_{ij} = \sum_{k=1}^{N} \overline{Q}_{ijk}(z_k - z_{k-1})$$
$$B_{ij} = \frac{1}{2}\sum_{k=1}^{N} \overline{Q}_{ijk}(z^2{}_k - z^2{}_{k-1}) \quad (7)$$
$$D_{ij} = \frac{1}{3}\sum_{k=1}^{N} \overline{Q}_{ijk}(z^3{}_k - z^3{}_{k-1})$$

In Eq. (7) the term z_k is the directed height of the k^{th} lamina with respect to the mid plane.

Substituting κ from Eq. (6) into following Eq. (8), dome height of laminate due to mechanical, thermal and piezoelectric effects can be obtained.

$$h = \frac{1}{\kappa}\left[1 - \cos\left(\frac{l\kappa}{2}\right)\right] \quad (8)$$

where h and l are the dome height and the length of a laminate.

2.2. Actuating parameters

As shown in Fig. 3, when a neutral plane by a new balance of thermal stress exists outside the PZT layer, the PZT layer subjected to electric fields contracts or expands in-plane direction. Thus asymmetrically laminated plate with PZT ceramic has a bending deformation. If only an electric field applies to PZT ceramic, bending moment per unit length in x and y directions can be written as functions of piezoelectric strain constants and electric fields.

$$M_x{}^{PZT} = aE^{PZT}d_{31}\Delta V$$
$$M_y{}^{PZT} = aE^{PZT}d_{32}\Delta V \quad (9)$$
$$M_{xy}{}^{PZT} = aE^{PZT}d_{12}\Delta V$$

where a is an actuation distance defined as the distance from the midpoint of PZT in the thickness direction to the neutral plane and the E^{PZT} is the elastic modulus of PZT. Since the polling direction is assumed to the thickness direction (d_{12}=0) of a laminate, $M_{xy}{}^{PZT}$ becomes zero.

When only an electric field applies to the PZT layer, Eq. (6) can be written as

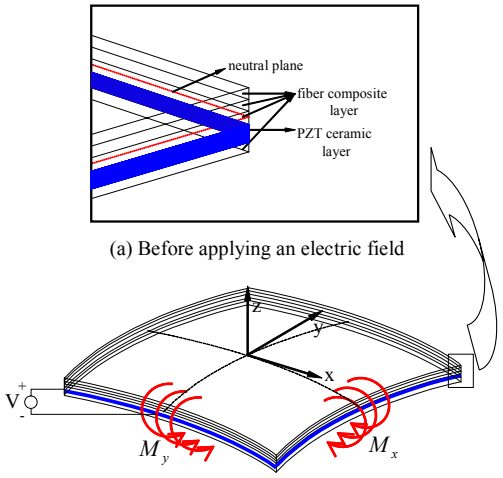

(a) Before applying an electric field

(b) After applying an electric field

Fig. 3. Actuating principle of a plate-type piezoelectric composite actuator subjected to electric field.

$$\begin{Bmatrix} \varepsilon^o \\ \kappa \end{Bmatrix} = \begin{bmatrix} A & B \\ B & D \end{bmatrix}^{-1} \begin{Bmatrix} N^{elec} \\ M^{elec} \end{Bmatrix} \quad (10)$$

If the bending moment by a piezoelectricity occurs in the laminated plate, the curvature of laminated plate is

$$\begin{bmatrix} \kappa_x \\ \kappa_y \\ \kappa_{xy} \end{bmatrix} = \begin{bmatrix} g_{11} & g_{12} & g_{16} \\ & g_{22} & g_{26} \\ sym & & g_{66} \end{bmatrix} \begin{bmatrix} M_x \\ M_y \\ 0 \end{bmatrix} \quad (11)$$

where g_{ij} is an inverse matrix of the bending stiffness matrix D_{ij}. Substituting Eq. (9) into Eq. (11) and assuming PZT to be a transversely isotropic material, Eq. (11) can be expressed as

$$\kappa_x = a(g_{11} + g_{12})E^{PZT}\Delta V d_{31}$$
$$\kappa_y = a(g_{12} + g_{22})E^{PZT}\Delta V d_{31} \quad (12)$$
$$\kappa_{xy} = a(g_{16} + g_{26})E^{PZT}\Delta V d_{31}$$

From the Eq. (12), the bending deformation of PCA subjected to electric field is affected by actuation distance, bending stiffness, elastic modulus of piezoelectric material, applied electric field and piezoelectric strain constant. Consequently, if elastic modulus, piezoelectric strain constants and electric field are constant, the flexural displacement of PCA is pro-

Table 1. Mechanical and piezoelectric properties used in finite element simulation.

Material properties	PZT ceramic (3203HD)	Carbon/ epoxy (woven fabric)	Glass/ epoxy (woven fabric)
Elastic properties			
E_{11} (GPa)	62	66.42	21.7
E_{22} (GPa)	62	66.42	21.7
G_{12} (GPa)	25.57	4.35	3.99
ν_{12}	0.31	0.054	0.13
Coefficients of thermal expansion			
α_1 (10^{-6}/°C)	3.5	0.16	14.2
α_2 (10^{-6}/°C)	3.5	0.16	14.2
Piezoelectric constant			
d_{31} (10^{-12}m/V)	-320	-	-
d_{32} (10^{-12}m/V)	-320	-	-
Thickness (mm)	0.25	0.105	0.07

portional to the actuation distance and inversely proportional to the bending stiffness.

3. Finite element analysis

To predict the flexural displacement of four kinds of model, PCA-A, PCA-B, PCA-C and PCA-D as shown in Fig. 2, a three dimensional finite element analysis (FEA) based on a thermal analogy (Taleghani et al., 1999) is performed with commercial code program ANSYS. Fig. 4 shows the model of PCA used in the analysis and the deformed shape after applying a thermal loading. The material properties used in the FEA are listed in Table 1. The element used is 8-node 3-D solid brick element with reduced integration is adopted for the FEA mesh, and a total of 15,360 elements are used. A perfect bonding condition is applied between fiber composite and PZT ceramic layers. The simulation for evaluating the flexural displacement of PCA consists of two steps. In the first step, a thermal deformation analysis is carried out to obtain the dome height of PCA caused by the temperature drop of -142℃ from the curing to room temperature. This step is a prerequisite procedure in order to more accurately predict the displacement performance in the PCA. In the second step, *z* directional flexural displacement of PCA under an electric field is calculated including the effect of thermal deformation obtained in the first step. In this step, continuous analysis function provided by ANSYS is used. For a loading condition, a constant electric field of 100 voltages (V) is applied to the only PZT ceramic layer in the thickness direction based on the thermal analogy. The used four kinds of boundary conditions (BCs) are illustrated in Fig. 5: (a) two edges simply supported (BC1), (b) four edges simply supported (BC2), (c) fixed-free (BC3) and (d) all-clamped (BC4). The flexural displacement is obtained at the apex of PCA for BC1, BC2 and BC4, and tip deflection of PCA is calculated for BC3.

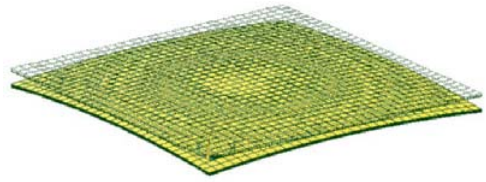

Fig. 4. The mesh configuration and the deformed shape of PCA after applying a thermal loading.

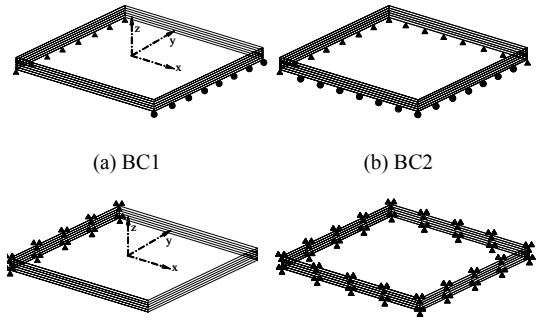

Fig. 5. Schematic of boundary conditions adopted in three dimensional finite element analyses: (a) 2-edge simply supported (BC1), (b) 4-edge simply supported (BC2), (c) fixed-free (BC3) and (d) all clamped (BC4).

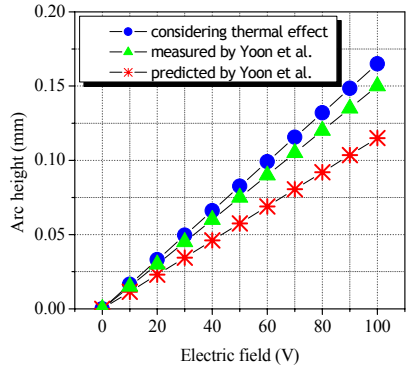

Fig. 6. Comparison of the arc height of LIPCA-C2 as a function of applied electric field.

4. Results and discussion

4.1. Effect of thermal deformation

In order to confirm the effect of thermal deformation, finite element simulation has been first applied for LIPCA-C2 (Yoon et al., 2004) actuator under the electric fields from 0 to 100 voltages at the simply supported boundary condition. Fig. 6 shows the arc height of LIPCA-C2 with and without the consideration of the effect of thermal deformation. At 100 V, the predicted value considering a thermal deformation shows 9 % difference compared to the measured one by Yoon et al., whereas the predicted one without the consideration of a thermal deformation shows 23 % difference compared to the measured one. Thus, it is noted that the effect of thermal deformation induced by a temperature change should be taken into account for more exact prediction of flexural displacement in the piezoelectric actuator.

4.2. The distribution of residual thermal stresses and thermally induced dome heights

In general, piezoelectric composite actuator undergoes a considerable temperature variation in the process of curing and then is exposed to a service temperature. In cooling process, internally induced thermal residual stresses take place discontinuously through the thickness of a laminate on account of the differences in coefficients of thermal contraction and in stiffness in the respective layer.

Figure 7 shows the distribution of thermal residual stresses and the locations of the neutral plane which is displayed in dotted line for asymmetrically laminated PCA as determined by the classical laminated plate theory. The neutral plane in Fig. 7 denotes a new balance of thermal stress induced by a thermal deformation. The temperature variation is assumed to be -142 ^{o}C that is a difference between curing temperature and room temperature. For every PCA, it is found that only tensile residual stresses occur in the glass-epoxy layers due to the material properties of glass-epoxy with a lower elastic modulus and a higher CTE compared with carbon-epoxy and PZT ceramic. Some tensile residual stress takes place along with compressive stress in the carbon-epoxy layer for PCA-A and PCA-D. It is also found that the stress

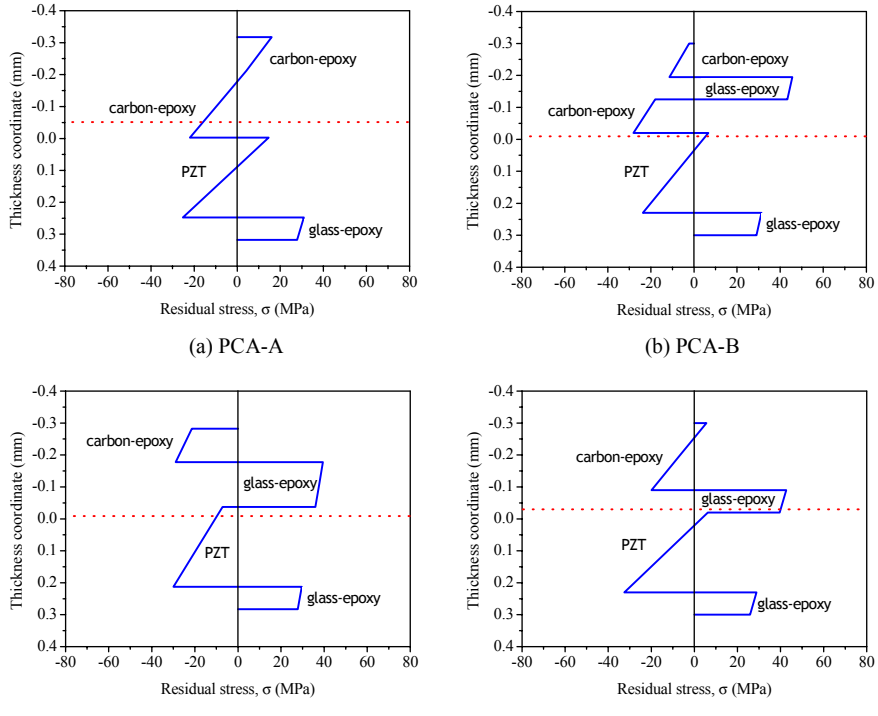

(a) PCA-A (b) PCA-B

(c) PCA-C (d) PCA-D

Fig. 7. The distribution of residual thermal stresses and locations of neutral plane in asymmetrically laminated plates with PZT ceramic layer.

gradient is considerably high at the interface of the PZT ceramic and the adjacent fiber composite layers. This stress gradient is a major factor of the failure in PZT ceramic, which was elucidated in the previous study (Woo et al., 2006b). In that the PZT ceramic has higher strength in compressive stress than in tensile one, it can be said that PCA-C where only compressive residual stress occurs in the PZT ceramic layer has a desirable lay-up sequence in a view of the integrity of actuator. One of the reasons why LIPCA-C2 actuator had the superior performance compared with THUNDER actuator is that the neutral plane after the curing process is located outside the PZT layer whereby the bending moment induced by the piezoelectricity for LIPCA-C2 actuator is much larger than that for THUNDER actuator. In this study, the neutral plane exists outside the PZT layer only in the case of PCA-A and PCA-D and thus it is suggested that PCA-A and PCA-D have a favorable lay-up sequence from a flexural displacement point of view.

Figure 8 shows the dome height induced by a pure thermal deformation as a function of the thickness of PZT. As the thickness of the PZT ceramic increases, the dome height of each PCA decreases and the decreasing degree is considerably different according to the lay-up sequence. In particular, the most pronounced diminishment occurs with PCA-C. For 0.05 mm, the value of dome height for PCA-C is 1.7 times as high as that of PCA-A; in contrast, for 0.3 mm, the value of dome height for PCA-C is twice lower than that of PCA-A. Such a difference in dome height according to lay-up sequence would have also affected the flexural displacement of PCA indicating that the proper selection of lay-up sequence can control the actuation distance and dome height of PCA.

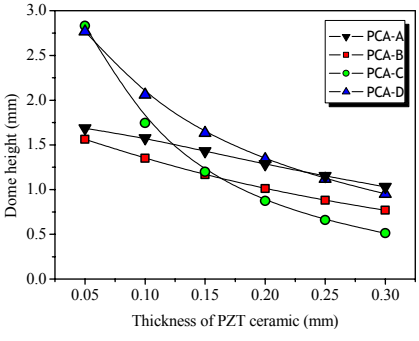

Fig. 8. The influence of PZT thickness on the thermally induced dome height for PCA.

4.3. Flexural displacement according to lay-up configuration

Figure 9 shows the results of the flexural displacement of PCA subjected to applied electric field of 100 V by FEA considering the effect of thermal deformation. From the figure, it is obvious that the decreasing tendencies in flexural displacement with increasing the thickness of PZT ceramic are similar to those for the dome height at the all BCs. Also, irrespective of the lay-up sequence, the value of displacement decreases under all BCs and its behavior varies in relation to the lay-up sequence. When the thickness of the PZT ceramic is 0.05 mm, PCA-C performs best under all BCs. For 0.1 mm, 0.15 mm, and 0.2 mm, PCA-D shows superiority. However, PCA-A exhibits the highest flexural displacement for 0.25 mm and 0.3 mm. This means that the thickness of the PZT ceramic considerably affects how the PCA performs in relation to the lay-up sequence and it is an important parameter in designing PCA. In general, shell structures are even stiffer as the curvature becomes more pronounced (Hazem et al., 2004). If so, the flexural displacement of PCA-A with the largest thermally induced dome height should have shown to be smallest when the thickness of PZT is 0.25 mm and 0.3 mm. However, PCA-A with a largest initial dome height exhibits a superior performance in this study. Therefore, it should be pointed out that the variations in actuation distance and bending stiffness of PCA have significant influence on the thermally-induced dome heights and flexural displacements of PCA. The results of Fig. 9 show that the use of thin PZT ceramic enhances the flexural displacement. Moreover, given that commercially available PZT ceramic has a thickness of 0.25 mm, it is suggested that PCA-A has the most desirable lay-up sequence within the study range.

4.4. Effect of PZT thickness on the bending stiffness and the actuation distance

From the Fig. 9 it was confirmed that the thickness variation of embedded PZT ceramic significantly affected the flexural displacement for the constant applied electric field. That is, as the thickness of the PZT ceramic increases, the bending stiffness and the actuation distance of PCA vary. Fig. 10 shows how the thickness of the PZT ceramic affects the bending stiffness and the actuation distance of PCA according

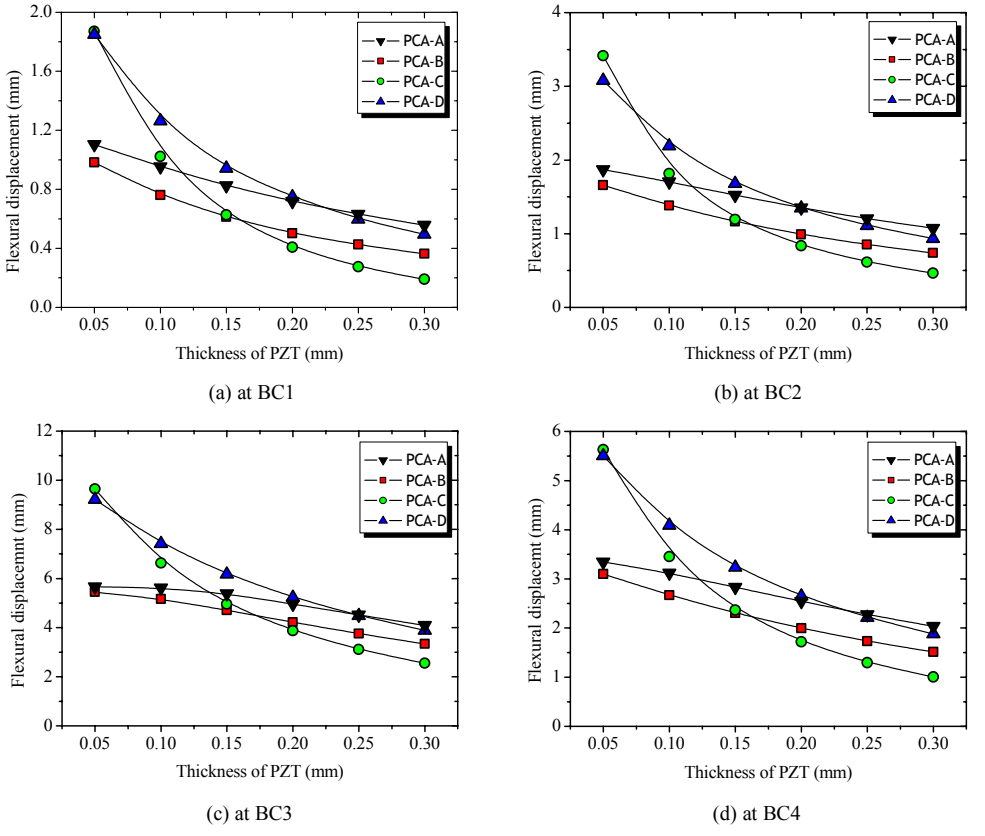

Fig. 9. Influence of PZT thickness on the flexural displacement at various boundary conditions subjected to an electric field of 100 V by finite element analysis.

to the lay-up sequence. Irrespective of the lay-up sequence, the bending stiffness of PCA increases due to the increment of thickness in embedded PZT ceramic. Furthermore, the extent of the increase is similar to one another but most obvious for PCA-A. In contrast, with increasing the thickness of the PZT ceramic, the actuation distance reveals a decreasing tendency in all lay-up types except for PCA-A, in which case the actuation distance shows a slight increase. In other words, the thick PZT ceramic leads to a rise in the bending stiffness of PCA irrespective of the lay-up sequence, but it does not always cause a decrease in the actuation distance because the actuation distance is directly dependent on the lay-up configuration. Although the actuation distance of PCA-A increases the value of flexural displacement decreases for all boundary conditions as shown in Fig. 9. The reason for this may be that the increasing degree in the bending stiffness of PCA-A is much larger than that in the actuation distance. Thus, it is concluded that the flexural displacement of PCA depends more on the bending stiffness than on the actuation distance.

5. Conclusions

In this article, the flexural displacement performance of a piezoelectric composite actuator with a thin sandwiched PZT plate with four kinds of lay-up configurations has been evaluated in association with the PZT thickness, bending stiffness, actuation distance and boundary conditions by three dimensional finite element analyses considering the effect of thermal deformation. The distribution of thermally-induced residual stress by a temperature drop has been also obtained. The results obtained are summarized as follows:

(1) By comparing the arc height for LIPCA-C2 with and without the consideration of thermal deformation effects, it is strongly recommended that the eff-

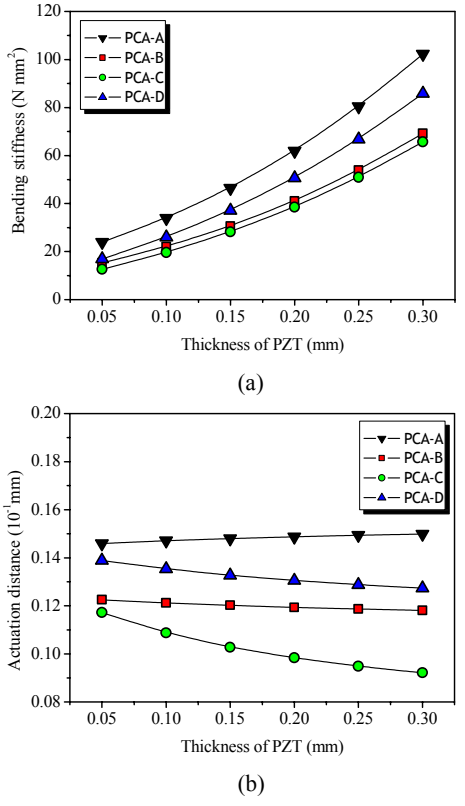

Fig. 10. Influence of PZT ceramic thickness on (a) the bending stiffness and (b) the actuation distance of PCA according to the lay-up sequence.

ect of thermal deformation should be considered for more exact displacement estimation of PCA.

(2) By investigating the distribution of the thermal residual stresses and the locations of the neutral plane, a desirable lay-up configuration for flexural displacement can be found within a study range.

(3) Irrespective of the lay-up sequence, the flexural displacements of PCA tend to decrease with the increase of the thickness of PZT ceramic; the reduction in the flexural displacement is due to the increase in the bending stiffness and the decrease in the actuation distance. Therefore, it is necessary to choose an adequate lay-up sequence and to select the proper thickness of PZT ceramic to produce a PCA with larger flexural displacement. Based on the results of the parametric studies, the actuating system composed of the upper layer with high modulus and low CTE and the lower layer with low modulus and high CTE is preferred for applications where large displacement is required.

Acknowledgements

The present work was supported by the Korea Research Foundation Grant (KRF-2006-005-J03302). The authors appreciate this financial support.

References

Cho, D. H., Lee, D. G., 1998, "Manufacturing of Cocured Hybrid Aluminum Composite Shafts with Preload to Reduce Residual Thermal Stresses," *Journal of Composite Materials*, Vol. 31, pp. 1221~1241.

Gex, D., Berthelot, Y. H., Lynch, C. S., 2005, "Low Frequency Bending Piezoelectric Actuator with Inte-grated Ultrasonic NDE Functionality," *NDT&E Inter-national*, Vol. 38, pp. 582~588.

Goo, N. S., Shin, S. J., Park, H. C., Yoon, K. J., 2001, "Design/Analysis/Manufacturing/Performance Evaluation of Curved Unsymmetrical Piezoelectric Composite Actuator LIPCA," *Transactions of KSME*, Vol. 25, pp. 514~1519 (in Korean).

Haertling, G. H., 1994, "Rainbow Ceramics-A New Type of Ultra-High-Displacement Actuator," *Bulletin of American Ceramic Society*, Vol. 73, pp. 93~96.

Haris, A., Goo, N. S., Park, H. C., Yoon, K. J., 2004, "Modeling and Analysis for the Development of Lightweight Piezoceramic Composite Actuators (LIPCA)," *Computational Material Science*, Vol. 30, pp. 474~481.

Hazem, K., Shaukat, M., 2000, "Piezoelectric Induced Bending and Twisting of Laminated Composite Shallow Shells," *Smart Materials and Structures*, Vol. 9, pp. 476~484.

Hellbaum, R., Bryant, R., Fox, R., 1997, Thin Layer Composite Unimorph Ferroelectric Driver and Sensor, US patent No. 5632841.

Hwang, W. S., Hwang ,W. B., Han, K. S., Park, H. C., 1993, "Active and Passive Control of a Laminated Composite Beam Using Piezoceramic Materials," *Transactions of KSME*, Vol. 17, pp. 485~491 (in Korean).

Kim, K. Y., Park, K. H., Park, H. C., Goo, N. S., Yoon, K. J., 2005, "Performance Evaluation Lightweight Piezo-Composite Actuator," *Sensors and Actuators A*, Vol. 120, pp. 123~129.

Liang, Y., Kuga, Y., Taya, M., 2005, "Design of Membrane Actuator Based On Ferromagnetic Shape Memory Alloy Composite for Synthetic Jet Applications," *Sensors and Actuators A*, Vol. 121. pp. 1~7.

Mossi, K., Green, C., Zoubeida, Z., Hughes, E., 2005, "Harvesting Energy Using a Thin Unimorph Prestressed Bender: Geometrical Effects," *Journal of Intelligent Material System and Structures*, Vol. 16, pp. 249~261.

Mulling, J., Usher, T., Dessent, B., Palmer, J., Franzon, P., Grant, E., Kingon, A., 2001, "Load Characterization of High Displacement Piezoelectric Actuators with Various End Conditions," *Sensors and Actuators A*, Vol. 94, pp. 9~24.

Taleghani, B. K., Campbell, J. F., 1999, "Non-Linear Finite Element Modeling of THUNDER Piezoelectric Actuators," *Smart Structure and Materials*, Vol. 3668, pp. 555~566.

Teymoori, M. M., Ebrahim, A. S., 2005, "Design and Simulation of a Novel Electrostatic Peristaltic Micromachined Pump for Drug Delivery Applications," *Senors and Actuators A*, Vol. 117, pp. 222~229.

Tzou, H. S., Zhou, Y. H., 1995, "Dynamic and Control of Non-linear Circular Plates with Piezoelectric Actuators," *Jounal of Sound and Vibration*, Vol. 188, pp. 189~207.

Wise, S. A., 1998, "Displacement Properties of RAINBOW and THUNDER Piezoelectric Actuators," *Sensors and Actuators A*, Vol. 69. pp. 33~38.

Woo, S. C., Goo, N. S., 2006a, "Influence of Applied Electric Fields and Drive Frequencies on The Actuating Displacement of a Plate-type Piezoelectric Composite Actuator," *Transactions of KSME*, Vol. 30. No. 5 pp. 576~584 (in Korean).

Woo, S. C., Goo, N. S., 2006b, "Analysis of the Bending Fracture Process for Piezoelectric Composite Actuators Using Dominant Frequency Bands by Acoustic Emission," *Composites Science and Technology*, in press. doi:10.1016/j.compscitech.2006.07.023

Woo, S. C., Park, K. H., Goo, N. S., 2007, "Influences of Dome Height and Stored Elastic Energy on the Actuating Performance of a Plate-type Piezoelectric Composite Actuator," *Sensors and Actuators A, in press.* doi:10.1016/j.sna.2007.01.018

Yoon, K. J., Park, K. H., Lee, S. K., Goo, N. S., Park H. C., 2004, "Analytical Design Model for a Piezo-Composite Unimorph Actuator and Its Verification Using Lightweight Piezo-Composite Curved Actuators," *Smart Materials and Structures*, Vol. 13, pp. 459~467.